

FLUID-STRUCTURAL ANALYSIS OF A NON-CONTACTING FINGER SEAL

Joury Temis, Alexey Selivanov, Ivan Dzeva
Central Institute of Aviation Motors (CIAM), Moscow, Russia
tejoum@ciam.ru

Keywords: *non-contacting finger seal, fluid-structure interaction (FSI), Reynolds equation, curved beam theory, clearance, leakage*

Abstract

Non-contacting finger seal models and calculation methods accounting for the deformation of seal elements under gas loading are developed. The developed models have different levels of detalization that enables us to use them both for fast preliminary calculations and for a full features analysis of the seal. Based on the developed models a calculation study of a finger seal is conducted and its efficiency and ability to proper operation is shown. Thus finger seals can be used for improving engine efficiency. Different constructive modifications of finger seal elements are considered.

1 Introduction

To reduce gas leakage through clearances between rotating and stationary parts in gas turbomachinery contacting or non-contacting seals are used.

The contacting seals create a region of the permanent contact between sealing parts which results in a full closure of radial clearance. They have very small leakage, however the friction leads to wear of the seals. The non-contacting seals have guaranteed clearance between the parts. The leakage rate is determined by the seal hydraulic resistance. Nevertheless the leakage through non-contacting seals is higher, they are widely used in gas turbines because of the great advantages – high reliability and long life-span.

For a long time the labyrinth seals have been the standard non-contacting type of seals. However, recently new air-to-air high-efficient seals (brush, finger, foil, leaf, etc.) have been

developed. They have low leakage and allow us to improve engine operating characteristics and to decrease specific fuel consumption.

The key issue for the developing of new seals is improving their sealing properties while maintaining the required life-span and reliability. One of the construction types satisfying these requirements are non-contacting finger seals. They operate due to the balancing of flexible fingers on a thin gas film above the shaft surface. The film thickness is very small, so leakage through the finger seal is to be 2-3 times lower than for a rigid labyrinth seal [1].

Obviously one needs to use the methods of multi-disciplinary mathematical simulation to account for the interaction between the gas flow and the flexible fingers. The current contribution is devoted to developing the models and methods for such an analysis on determining finger seal characteristics. Based on the calculations the operation of the finger seal is analyzed and different constructive modifications for improving the seal's efficiency and ability to proper operation are considered.

One approach to perform such an analysis is to solve a corresponding aeroelasticity problem by means of detailed coupled 3D finite element method and finite volume method models [2-3]. This approach is usually very time-consuming both from the point of preparing numerical models and computations as well. In the present work we used computation-effective methodology of finger seal static and dynamic parametric study. This approach was proposed in [4] and is based on simplified approaches: curved shape beam

model is used for stress-strain finger analysis and 2D Reynolds model is used for gas flow simulation and calculation of gas forces acting on the lift pads.

2 Finger seal assembly

A typical assembly of the finger seal is comprised of a stack of plates fixed along the outer diameter (Fig. 1).

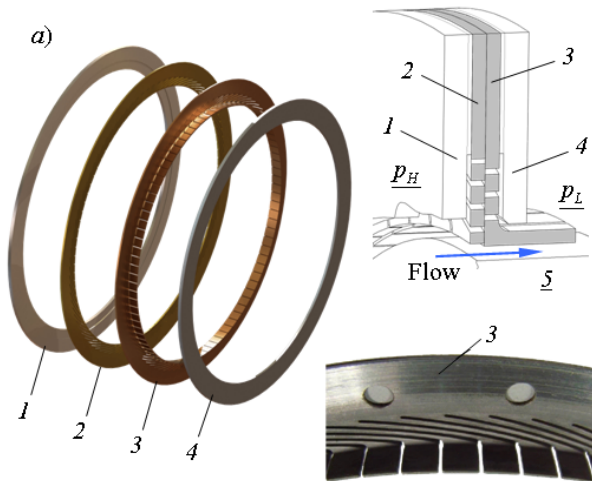


Fig. 1. A non-contacting finger seal assembly: 1 – front plate of the case; 2 – upstream plate with padless fingers; 3 – downstream plate with padded fingers; 4 – back plate of the case; 5 – rotor

The thick plates of the case typically have spacers with or without pressure dam. The thinner central plates (laminates) have uniform cuts forming separated flexible elements of the seal (“fingers”). When the seal is assembled, the central laminates are rotated around each other in such a way that the fingers of the upstream laminate close the cuts in the downstream one (a staggered configuration of fingers is established), thus preventing the direct leakage through the seal.

The downstream fingers have special lift pads extended only to the low pressure zone [1]. These pads provide a potential for fingers to adjust the clearance in the seal by deflecting as cantilever beams with respect to external seal kinetics. So gas leakage is to be significantly lower than for rigid labyrinth seals being non-compliant and thus forced to have a rather large operating clearance.

The key factor for providing the proper operability of the non-contacting finger seal is

the balancing of the fingers in the gas flow. The principle of such balancing is based on the arising of gas-static and gas-dynamic pressure in the gap under the pads. Induced gas forces achieve the equilibrium with elastic reaction forces, caused by the deformation of fingers, and the external pressures in the cavities.

Tuning the seal for the required range of radial displacements is possible by controlling both the stiffness of fingers (via changing their shape or laminate material) and acting aerodynamic lifting force (via designing the shape and additional features of the gap under pads). The appropriate choice and arrangement of all seal parameters, including the choice of initial clearance, allows to ensure the contactless operation of the seal with small clearance on different engine regimes.

3 Finger seal model

The model of a whole finger seal is developed on the basis of a characteristic (repetitive) “cell” of the seal. To predict fingers’ radial displacements caused by passing gas flow (and thus seal operating clearance) it is sufficient to consider the cell consisting of an arbitrary padded aft-finger, two halves of adjacent padless fore-fingers and a thin gas film in the gaps between the pad and foot portions of fingers and shaft surface.

A schematic of a finger seal analysis algorithm accounting for the deformation of seal elements under gas loading is shown in Fig. 2.

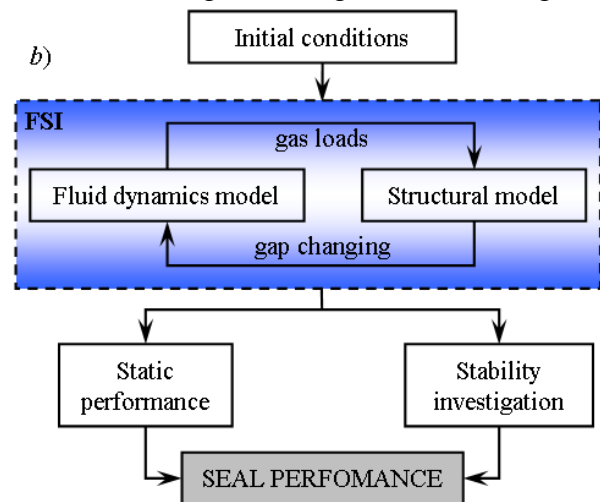


Fig. 2. Schematic of a finger seal analysis algorithm

3.1 Gas flow model

Because ratio h/R_{sh} of a gap thickness (clearance) h to a shaft radius R_{sh} is small enough (about 10^{-4}), we can neglect curvature of gap shape and consider its involute with the base D_{inv} on the rotor surface (see Fig. 3). In order to determine gas flow parameters in such gaps with very small h we can use Reynolds assumption for a thin gas layer, which is widely used for hydrodynamic seals and bearings analysis [5,6].

In this simplified model, pressure distribution $p = p(z, s, t)$ is constant through the gap thickness and is determined by 2D unsteady Reynolds equation [4-6]:

$$\begin{aligned} \frac{\partial}{\partial z} \left(h^3 p^\alpha \frac{\partial p}{\partial z} \right) + \frac{\partial}{\partial s} \left(h^3 p^\alpha \frac{\partial p}{\partial s} \right) = \\ = 12\eta \frac{\partial (hp^\alpha)}{\partial t} + 6\eta\omega R_{sh} \frac{\partial (hp^\alpha)}{\partial s} + p^\alpha G, \end{aligned} \quad (1)$$

$(z, s) \in D_{inv}, t > 0,$

where $h(z, s, t)$ is the gap thickness (clearance); $\alpha = 1/\gamma$, γ is adiabatic exponent; η is dynamic viscosity; ω and R_{sh} are an angular velocity

and a radius of the rotor; G accounts for sources and sinks in the gap; z and s are axial and circumferential local Cartesian coordinates on the gap involute D_{inv} . In Eqn. (1) gas inertia effects are neglected and flow is treated to be compressible, adiabatic, laminar, with constant viscosity $\eta = \text{const}$ (calculated at the specified temperature).

On the boundaries of computational region we set static pressures values: in the inlet $p = p_H$ and in the outlet and circumferential sides $p = p_L$. Here $p_L = p_H - \Delta p$, where Δp is an axial pressure drop across the seal. As the initial condition for transient simulation we use constant atmospheric pressure or steady state pressure distribution $p_{st}(z, s)$.

In 2D case with accounting circumferential flow solution is found numerically by using the in-house unsteady nonlinear FEA program based on implicit Euler scheme of the in time integration and Newton-Raphson method. The Reynolds equation (1) was made dimensionless [6] to get good convergence of each time step solution.

Developed simplified 2D model based on Reynolds equation (1) is successfully verified by comparing with 3D CFD results [4].

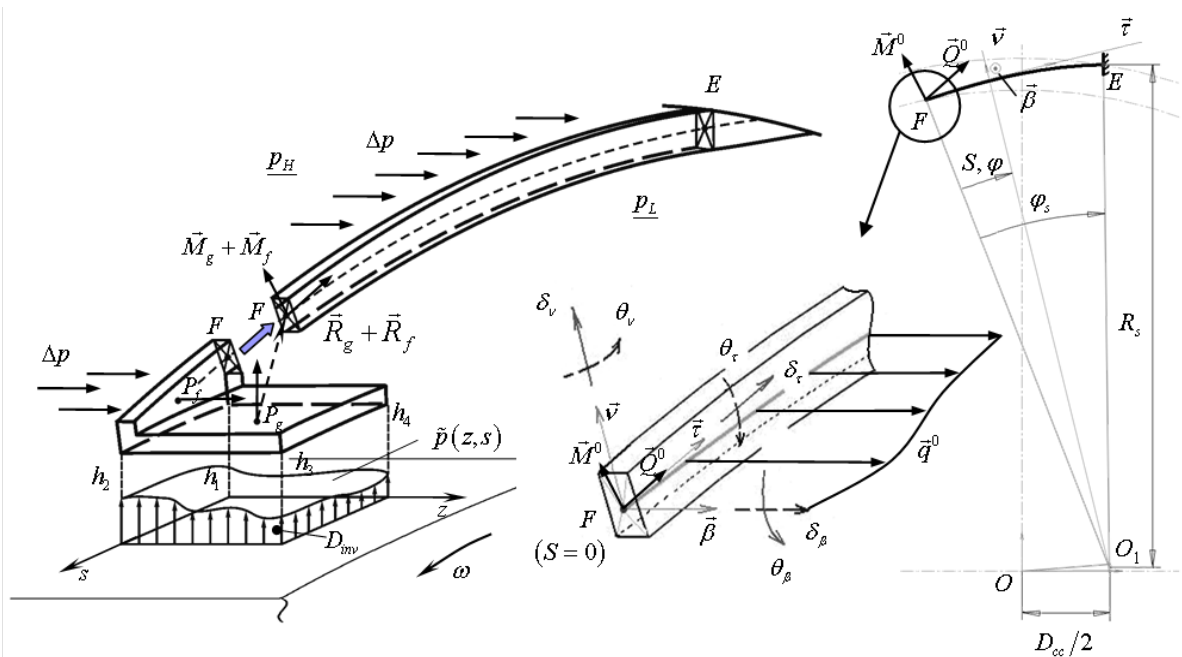


Fig. 3. Finger seal characteristic (repetitive) cell and schematic of the finger beam model (padless fore-fingers are not shown; gap is shown magnified)

3.2 Structure model

In the finger stress-deformed model the stick of the finger is represented as a flexible cantilever beam while the lift pad is assumed a rigid body [4].

Equivalent gas flow loads (force and moment) in the gap are applied to the end cross-section of the beam. Distributed load depending on axial pressure drop and contact pressure among fingers is applied over the length of the beam. The internal forces and moments in all cross-sections of the beam are calculated from equilibrium equations of a beam with arbitrary curved axis.

Then the motion of end cross-section (F) of finger stick is calculated by using the Mohr's integrals

$$\Delta_i = \int_0^{\varphi_s} \left(\frac{M_1 M_1^{\Delta_i}}{E_s J_\beta} + \frac{N N^{\Delta_i}}{E_s S_s} + k_v \frac{Q_1 Q_1^{\Delta_i}}{G_s S_s} \right) R_s d\varphi, \quad i = 1, 2, 3;$$

$$\Delta_i = \int_0^{\varphi_s} \left(\frac{M_2 M_2^{\Delta_i}}{E_s J_v} + \frac{M_t M_t^{\Delta_i}}{G_s J_t} + k_\beta \frac{Q_2 Q_2^{\Delta_i}}{G_s S_s} \right) R_s d\varphi, \quad i = 4, 5, 6,$$

where corresponding unit forces and moments are denoted by index Δ_i , $J_{(\cdot)}$, $k_{(\cdot)}$ and S_s are stick cross-section parameters, E_s and G_s are elasticity modules.

The beam model results are successfully verified by 3D detailed FEA calculations [4].

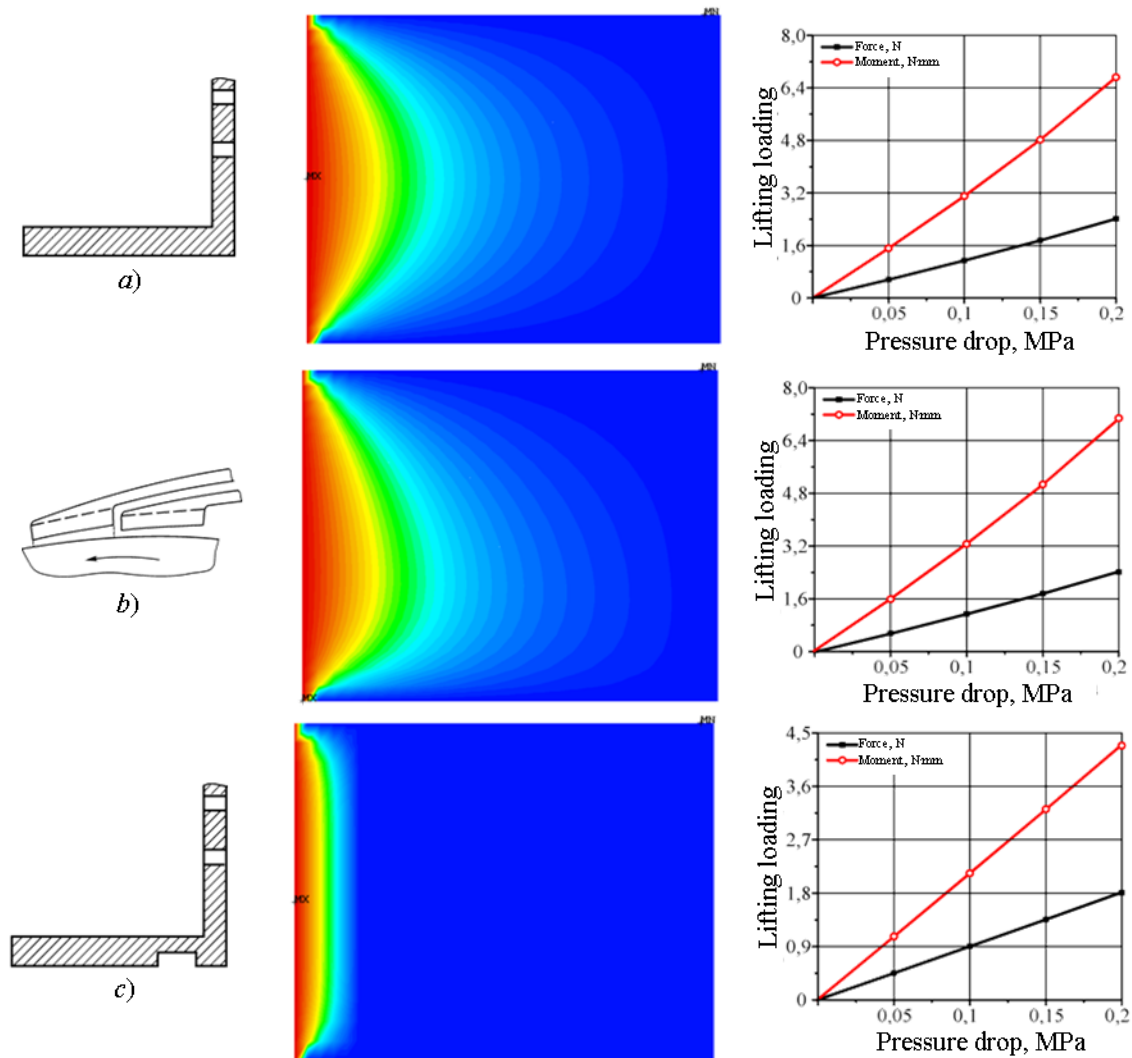


Fig. 4: Pressure distribution and lifting loading for different designs of lift pad
 a – typical smooth pad; b – inclined pad; c – grooved pad

4 Results

After successfully verifying developed gas-dynamic model we use it to investigate different design features of the finger pad. Fig. 4 represents pressure distributions and lifting loadings (force and moment) versus pressure drop for finger seals with typical smooth lift pads (Fig. 4,a), inclined (in circumferential direction) pads (Fig. 4,b) and with grooved pads (Fig. 4,c). In all cases gas leakage for finger seal is several times lower than for typical labyrinth seal.

As seen in the Fig. 5 the aerodynamic loads are highly non-linear in the range of small clearances, meanwhile they are practically constant at large clearances (this likely due to setting static pressures on the boundaries). The influence of the pad inclination on the lifting force is noticeable at small clearances – developing either a gas-dynamic build-up in a circumferentially converging film ($h_1 > h_2$, see Fig. 3), or a «suction» force otherwise ($h_1 < h_2$) (see also [6]). It is should be noted that gas force and gas moment have qualitatively similar distributions.

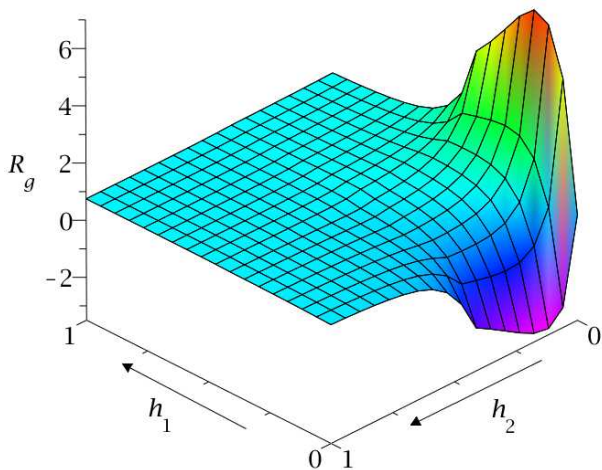


Fig. 5. Gas lifting force distribution versus clearance shape normalized parameters (see Fig. 3)

Typical deformed state of standalone padded aft-finger is shown in the Fig. 6.

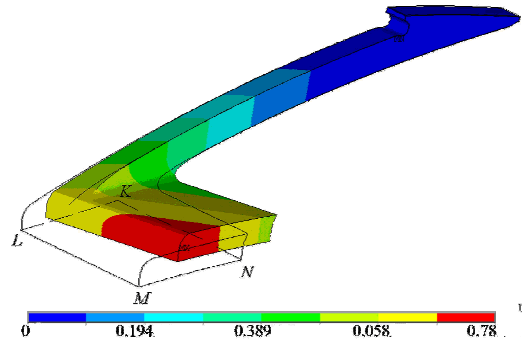
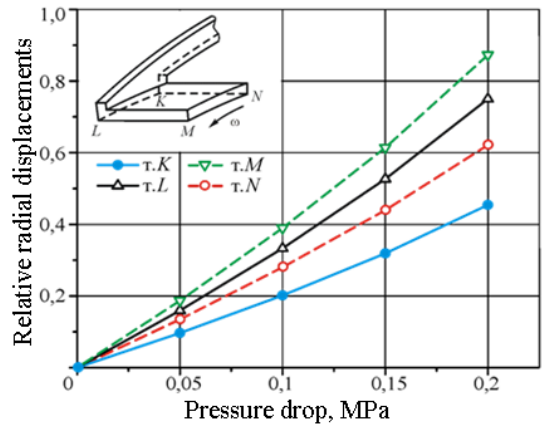
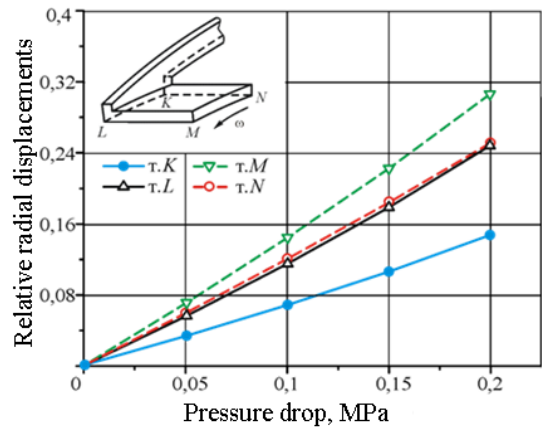


Fig. 6. Relative (to initial gap) displacements of padded finger

Fig. 7 shows relative (to initial gap) radial displacements of the fingers for two seals – with inclined pads and with grooved pads. Gas loads for these seals were calculated above (see Fig. 4). As it can be seen we can change the lift force (and moment) widely by using different design features of the seal (or pads).



a)



b)

Fig. 7. Relative (to initial gap) radial displacements of the fingers versus pressure drop: a – with inclined pads; b –with grooved pads

5 Example of preliminary finger seal design

Finally a simple iterative algorithm is developed to solve inverse problem of mathematical simulation and to design a new finger seal, satisfying the specified requirements for the radial displacement of the pads.

In fact our aim through the design procedure is to find a set of finger seal geometric parameters which determine a finger with correct stiffness. We can estimate stiffness of a finger stick by simple relation

$$k_{stick} \sim E_s W_s \left(\frac{H_s}{L_s} \right)^3. \quad (2)$$

Equation (6) is derived applying the methods of strength-of-materials for a straight cantilever beam with the constant cross-section loaded on its free end by a concentrated force. In the design procedure we use stiffness ratio so this simplest relation (which indeed only approximates the actual finger stiffness) allows obtaining the desired results. Afterwards these are verified by 3D detailed FEM simulation accounting contact interaction.

First, we investigate the influence of increasing pad circumferential length on the leakage through the seal (Fig. 11). Then, we solve inverse problem for updated construction to determine appropriate stiffness of fingers.

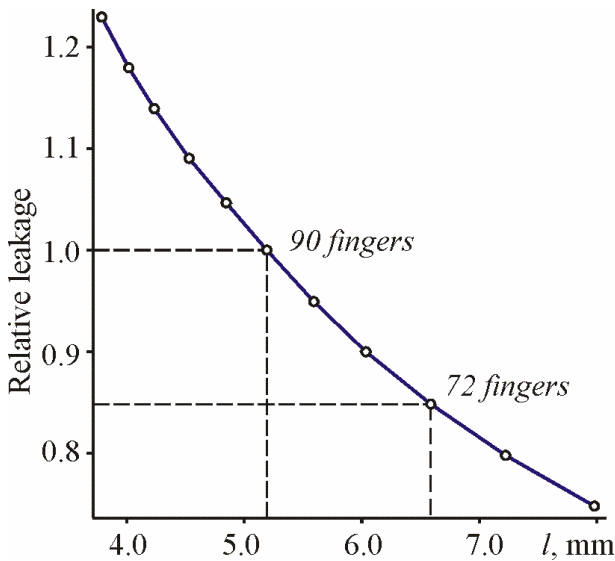


Fig. 8. Relative leakage versus pad circumferential length

The variation of height of stick cross-section H_s is usually constrained (vary not considerably). Thus, formula (2) shows that we can control stiffness of a finger in wide range by choosing material (with elasticity module E_s) and width of plates W_s , and varying finger length L_s , which is determined by a group of design parameters.

The flow-chart of the finger seal design overall algorithm can be found in [4]. The key moment is comparing different sets of finger seal design parameters by ratio of stick stiffness and utilizing the estimate (2).

Detailed 3D FEM model accounting contact interaction between seal laminates was developed for final verification. Results shown in Fig. 9 demonstrate that the designed new seal geometry satisfies specified requirement for radial displacements of fingers (values d_r belong to 1...2 interval in relative to initial gap terms).

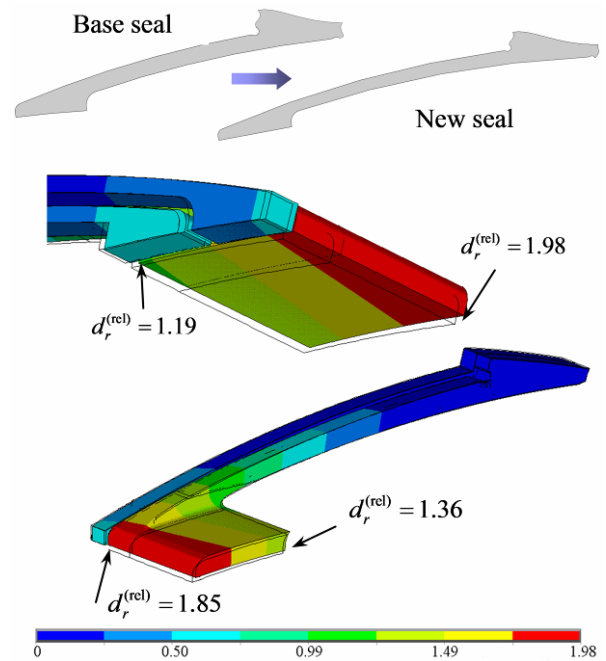


Fig. 9. Relative (to initial gap) radial displacements of the designed seal [4]

6 Conclusion

The non-contacting finger seal, first of all, should be considered as a compliant system, capable to response on the clearance changing in the seal, caused by external factors.

The fingers are balanced in the gas flow by means of the spring force of their sticks and two components of gas lifting force. The first one (a gas static force) is determined by an axial pressure drop and is responsible for a base deflection of fingers. The second one (a variable gas dynamic force) arises due to a shaft rotation and establishes a possibility of correct deflection of fingers when the clearance is changing.

A fully parametric and computations saving models, methods and tools for analysis and design of a high-efficient finger seal are developed.

References

- [1] Proctor M. and Delgado I. Preliminary Test Results of a Non-Contacting Finger Seal on a Herringbone-Grooved Rotor. NASA/TM-2008-215475, AIAA-2008-4506, 22 p., 2008.
- [2] Braun M., Pierson H. and Deng D. Thermofluids Considerations and the Dynamic Behavior of a Finger Seal Assembly. *Tribology Transactions*, 48(4), pp. 531-547, 2005.
- [3] Zhang H., Zheng Q. and Yue G. Study on the Leakage and Deformation Characteristics of the Finger Seals by Using Numerical Simulation. *Proc. ASME Turbo Expo 2010*, Glasgow, UK, June 14–18, Paper GT2010-23194, 12 p., 2010.
- [4] Temis J., Selivanov A. and Dzeva I. Finger Seal Design Based on Fluid-Solid Interaction Model. *Proc. ASME Turbo Expo 2013*, San-Antonio, Texas, USA, June 3-7, Paper GT2013-95701, 9 p., 2013.
- [5] Pinkus O. and Sternlicht R. (1961): *Theory of Hydrodynamic Lubrication*. McGraw-Hill, New York.
- [6] Galimutti P.P., Sawicki J.T. and Fleming D.P. (2009): Analysis of finger seal lift pads. In *Proc. ASME Turbo Expo 2009*, Orlando, Florida, USA, June 8–12, Paper GT2009-59842, 10 p.

Copyright Statement

The authors confirm that they, and/or their company or organization, hold copyright on all of the original material included in this paper. The authors also confirm that they have obtained permission, from the copyright holder of any third party material included in this paper, to publish it as part of their paper. The authors confirm that they give permission, or have obtained permission from the copyright holder of this paper, for the publication and distribution of this paper as part of the ICAS 2014 proceedings or as individual off-prints from the proceedings.